Shear Instability of γ-Fe in Bulk and in Ultrathin Films

D. Spišák and J. Hafner

Institut für Materialphysik and Center for Computational Materials Science, Universität Wien, Sensengasse 8/12, A-1090 Wien, Austria

(Received 22 May 2001; published 16 January 2002)

Using *ab initio* local-spin-density calculations we demonstrate that along the Bain path describing the transformation of face-centered-cubic (fcc) γ-Fe into body-centered-cubic (bcc) α-Fe, tetragonal Fe is unstable against monoclinic shear deformations producing a nearly bcc structure. In the limit of a monolayer adsorbed on a fcc substrate, the epitaxial constraint suppresses the shear instability, but in ultrathin films with three to six monolayers a striped pattern of near-bcc domains develops, confirming recent observations by scanning tunneling microscopy. A strong correlation between the shear instability and the magnetic state is reported.

DOI: 10.1103/PhysRevLett.88.056101 PACS numbers: 68.55.–a, 75.70.Ak

Ultrathin magnetic films exhibit properties that may differ significantly from those of the corresponding bulk materials. These differences are caused mainly by the increasing influence of the reduced dimensionality with decreasing film thickness and by the strain induced by the epitaxial constraint at the interface. Fe films grown on Cu(100) substrates have attracted particularly widespread interest as a model system for studying the correlation between atomic structure and magnetism [1–8].

Up to a thickness of about 10–11 monolayers (ML) the pseudomorphic growth on the Cu substrate stabilizes the face-centered-cubic (fcc) γ phase of Fe, which exists in the bulk only at temperatures above 1186 K. The density of the epitaxially grown Fe films is very close to the range for which a spin-wave instability has been predicted for bulk γ-Fe [9]. At these densities ferromagnetic (FM) low- and high-spin states, antiferromagnetic (AFM), and nonmagnetic phases differ only very little in energy and it is therefore not surprising that the structural and magnetic ground state of Fe/Cu(001) depends critically on film thickness and growth conditions. During the last decades, hundreds of experimental and theoretical studies have been devoted to this intriguing system. Finally, at least for room-temperature-grown films, for which layer-by-layer growth can be achieved, this vast research effort seemed to converge upon a consistent picture: (i) Films with up to 3–4 ML are ferromagnetic; the structure is tetragonally distorted fcc [2–4] and shows a considerable three-dimensional lattice modulation [5] with (1×4) or (1×5) periodicity. (ii) At thicknesses ranging from 4–5 to about 11 ML the Fe films have been characterized as isotropically fcc on average and antiferromagnetic [6–8], with a small net magnetic moment due to a FM coupling of the enhanced moments in the surface and subsurface layers. For films with about 6 ML a (1×2) reconstruction has been reported. (iii) At thicknesses above 11 ML, the films transform to the body-centered-cubic (bcc) structure stable in bulk Fe.

Local-spin-density (LSD) calculations performed in the generalized-gradient approximation have contributed considerably to clarify the structural and magnetic phase diagrams of Fe/Cu(001) films [10–14]. The calculations explain the FM state of films in regime (i) and their tetragonal distortions as resulting from a magnetovolume effect. In regime (ii) AFM structures are predicted, with a bilayer sequence ($\uparrow\uparrow\downarrow\downarrow \ldots$) of the spin orientations for films with an even number of ML. Interlayer distances between FM coupled layers are expanded; AFM coupling leads to contracted spacings so that the structure is fcc on average. The most recent work [14] even explains the observed complex reconstructions as resulting from the interplay between the enhanced surface moments and the correlated local expansions. However, certain small discrepancies between theory and experiment remained, concerning, in particular, the distance between surface and subsurface layers.

Very recently, this seemingly well established picture has been challenged on a very elementary level [15]. Using scanning tunneling microscopy (STM) with atomic resolution it was observed that in regime (ii) bcc nucleation centers appear as long needlelike crystals which had been described also in earlier studies [16]. Within the needles, atomic rows are tilted with respect to the underlying fcc lattice but appear to be perfectly lattice matched along both sides. The tilt angle is smaller than 19.5° corresponding to an ideal bcc layer on a fcc substrate. In regime (i) a large portion of the surface of the film is covered by a zigzag pattern with $(1 \times n)$ periodicity, $n = 4–6$. In analogy with the needles found in the thicker films, this structure has been described as consisting of stripes with a local bcc structure. All structures can be considered as resulting from a monoclinic shearing of the fcc lattice by $\pm 14°$ such that the local atomic configuration is very similar to that of a (110) bcc film in the Pitsch orientation with respect to the (001) fcc substrate [17]; see Fig. 1. Films with about 3 ML show the highest content of "bcc-like" stripes, whereas films with 2 or 5 ML show a higher fcc content. The fact that the highest content of local bcc arrangement is found at the film thickness with the highest magnetization has been interpreted as representing the strong correlation between a bcc-like structure and its magnetic state. While

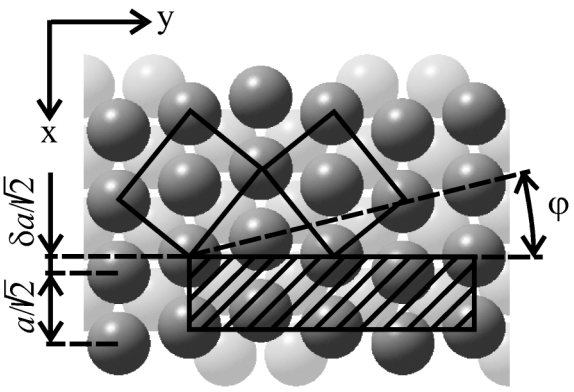

FIG. 1. Two topmost layers of the (1×4) "striped bcc" reconstructed structure on top of the underlying fcc structure of the substrate. The hatched rectangle shows the (1×4) surface cell; the smaller rectangles mark the strained (110) bcc-like cells. The shear angle φ of 14° is that measured in the STM experiment; the present calculations predict a shearing by 13° for a film of 3 ML Fe/Cu(100). δ and a are the lateral shift parameter and cubic lattice constant of substrate, respectively.

(1×4) periodicity is compatible with the earlier LEED observations, the lateral shifts of the atoms estimated from the STM picture (± 0.65 Å corresponding to about a quarter of the surface lattice constant) are distinctly larger that the amplitude of the sinusoidal lateral modulation derived from LEED [5] or calculated in the LSD approximation [14]. However, it should not be forgotten that the lateral resolution of LEED is quite limited.

In this work we return to the question of the stability of γ-Fe in the bulk and in ultrathin films from the point of view of *ab initio* local-spin-density calculations. In our previous work [14] we have analyzed the total energy of the FM and AFM phases (including both single and double layer sequences of spins) of tetragonal Fe as a function of lattice parameters a and c. It was shown that for all three magnetic phases the minimum in the total energy occurs for a tetragonal structure—even for the FM phase which can have cubic symmetry. It was also demonstrated that the structure of the FM Fe/Cu(001) films in regime (i) and of the AFM films in regime (ii) correlated very well with the bulk structure of tetragonal γ-Fe. In the present work we extend these studies by allowing shears along the [100] direction in the (001) plane. The surprising result is a shear instability of tetragonal γ-Fe, irrespective of the magnetic state. We also investigate the formation of bcc-like stripes in ultrathin films and find it to be energetically favored.

Our calculations have been performed using the spin-polarized version of the Vienna *ab initio* simulation package, VASP [18]. VASP performs an iterative solution of local-spin-density theory on the basis of projector-augmented waves [19]. The exchange-correlation functional of Perdew and Zunger [20] with the spin interpolation of Vosko, Wilk, and Nusair [21] and the generalized-gradient corrections of Perdew *et al.* [22] have been used. Structural relaxations have been performed using a quasi-Newton algorithm and the exact Hellmann-Feynman forces acting on the atoms. The model for ultrathin films consists of three Cu substrate layers plus a variable number of Fe layers followed by six vacuum layers. The two deeper layers of the Cu substrate were fixed in an ideal fcc structure with the equilibrium lattice constant of bulk fcc Cu [a_{Cu}(theor.) = 3.637 Å; a_{Cu}(exp.) = 3.61 Å]. Convergence with respect to plane-wave cutoff and $\vec{k}$ points sampling was carefully checked.

Figure 2 shows the total energy of FM Fe as a function of the shear parameter δ and c/a ratio for $a = 3.40$ Å. The structure is defined by the basis vectors $\vec{a}_1 = a/\sqrt{2}\,(1,0,0)$, $\vec{a}_2 = a/\sqrt{2}\,(\delta,1,0)$, $\vec{a}_3 = a(0,0,c/a)$ together with the atomic positions $\vec{A}_{2i} = (0,0,i)$ and $\vec{B}_{2i+1} = (1/2,1/2,i+1/2)$ given with respect to the basis vectors. An ideal fcc structure is realized for $\delta = 0$ and $c/a = 1$. As long as the atomic rows parallel to the [100] direction remain in commensurate positions with the fcc lattice, a complete transformation to an ideal bcc structure can be achieved only along the epitaxial Bain path $\delta = 0$, $c/a = 1 \rightarrow 1/\sqrt{2}$. For $\delta \neq 0$ the sheared fcc structure will approach the bcc configuration, but the structure will always remain strained along the [100] direction. We find that at all lattice parameters ranging between $a = a_{\mathrm{Cu}} = 3.637$ Å and $a = 3.400$ Å minimizing the total energy of ferromagnetic Fe in an assumed face-centered-tetragonal (fct) structure, Fe is unstable against both tetragonal and monoclinic shears. At $a = a_{\mathrm{Cu}}$, related to thick Fe films on Cu(001), the tetragonal distortion is very small ($c/a = 1.009$) and the minimum energy structure at $\delta = 0.259$ corresponds to the shear angle $\varphi = 14.5°$; the energy gained with respect to the ideal fct lattice is $\Delta E = 90$ meV/atom. At a smaller in-plane lattice constant both the tetragonal and the monoclinic shear increase. The tetragonal energy minimum identified in our earlier work corresponds to a saddle point on the potential energy surface. Similar but more modest shear instabilities are found in all magnetic phases. At $a = a_{\mathrm{Cu}}$ we find energy minima at $c/a = 0.900$, $\varphi = 2.6°$ for paramagnetic, $c/a = 0.967$, $\varphi = 4.4°$ for single layer AFM, and $c/a = 0.993$, $\varphi = 7.3°$ for bilayer AFM Fe. This

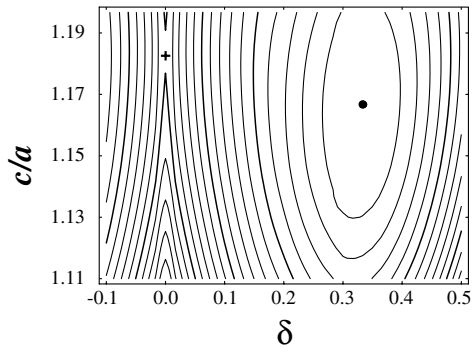

FIG. 2. Contour plot of the total energy per atom of ferromagnetic Fe as a function of δ and c/a, for $a = 3.40$ Å. The energy minimum along the epitaxial Bain path is marked by a cross ($c/a = 1.18$, $\delta = 0$), the absolute minimum by a full dot. The contour interval is 10 meV.

confirms that the tendency towards a bcc-like distortion is indeed correlated with FM ordering. For $a = a_{\mathrm{Cu}}$, the FM phase is 45 meV/atom lower in energy than the bilayer AFM configuration, 120 meV/atom than the single layer AFM, and 145 meV/atom than the paramagnetic phase. If the cell shape is constrained to tetragonal symmetry, a bilayer AFM phase with $c/a = 1.00$ and a FM phase with $c/a = 1.05$ are energetically almost degenerated at this lattice constant [14]. The analysis of the spin-polarized electronic density of states (DOS) reveals the strong similarity of DOS of the sheared fcc phase with that of bcc Fe. In particular, one observes the bonding-antibonding splitting characteristic for the bcc phase and absent in γ-Fe.

In the next step we examine whether the shear instability exists also in thin films or if it is suppressed by the epitaxial constraint. The calculations are performed for a (1×4) surface cell with the zigzag displacement pattern of the atoms in the top layer. Atoms in a four-atom surface cell are displaced by 0, $-\delta a_{\mathrm{Cu}}/\sqrt{2}$, 0, $+\delta a_{\mathrm{Cu}}/\sqrt{2}$ in the x direction, the y coordinate is fixed, and the z coordinate is allowed to adjust such as to minimize total energy; cf. Fig. 1. For the atoms in the deeper layers, including the top layer of the substrate only the y coordinate is fixed; x and z are allowed to relax. Figure 3 displays the the total energy of an Fe monolayer on Cu(001). It increases monotonically with δ. Hence the coupling across the interface is strong enough to stabilize the adsorbed Fe monolayer against shearing. Figure 3 shows also the total energy of a film consisting of 3 ML of Fe—evidently the Fe film is unstable against shearing; the energy minimum is found at $\delta = 0.23$, corresponding to a shift by 0.59 Å and a shear angle of 13° in excellent agreement with the shear angle of 14° deduced from the STM experiment. The shear deformation is accompanied by a slight buckling of the surface by $\Delta z = 0.05$ Å. On average, the first interlayer distance is contracted by 1.8%. Unlike the experiment, the computer simulation also yields precise information on the structure of the deeper layers. Figure 4(a) shows the lateral displacements of the atoms in the two deeper Fe layers and in the first Cu layer. Already in the first subsurface Fe layer the lateral displacement is reduced to about half its value in the top layer, but even the Cu substrate still undergoes a small deformation. Evidently, the structure of the film is a compromise between the magnetically driven distortion and the restoring forces from the bonding to the Cu substrate. The epitaxial constraint is also important for restricting the width of the bcc-like domains: As the subsurface layers follow the shear distortion only to a limited degree [$\delta(S-1) \leq 0.5\delta(S)$, $\delta(S-2) \leq 0.3\delta(S)$; cf. Fig. 4(a)], only alternating shifts according to 0, $-\delta a/\sqrt{2}$, 0, $+\delta a/\sqrt{2}, \ldots$ resulting in a (1×4) structure or eventually 0, $-\delta a/\sqrt{2}$, $-\delta a/\sqrt{2}$, 0, $+\delta a/\sqrt{2}$, $+\delta a/\sqrt{2}, \ldots$ producing a (1×6) domain pattern lead to structures that put not too much strain on the bonds between surface and subsurface atoms. If the layers of a film are allowed to relax also in the y direction, the largest shift occurs in the $(S-1)$th layer, $\Delta y = \pm 3.4\%$ of the ideal in-plane bonding distance. In addition, the vertical buckling amplitude increases to $\Delta z = 0.18$ Å, in good agreement with the buckling deduced from the LEED analysis [5,23]. Hence the reconstruction of the films is fully three dimensional.

In bulk FM Fe at $a = a_{\mathrm{Cu}}$, shearing decreases the energy by 90 meV/Fe atom; the energy increase of a comparable deformation in an adsorbed Fe monolayer is about 50 meV/atom. For a 3 ML Fe film the formation of the striped bcc (1×4) phase results in an energy lowering by 13 meV/Fe atom. We also remark that this energy gain is comparable to, but a bit larger than, the energy gain calculated in our previous work on unconstrained (1×4)

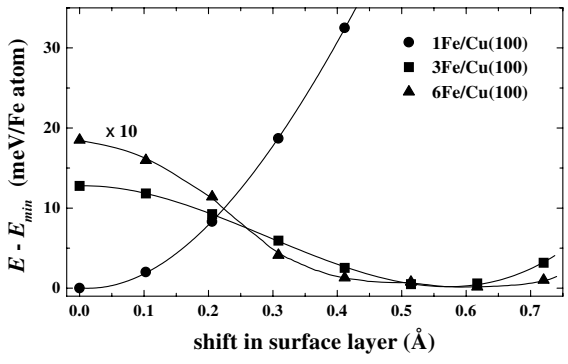

FIG. 3. Total energy of a monolayer of Fe (circles), of a 3 ML film (squares), and of 6 ML film (triangles) adsorbed on Cu(100) as a function of the shear deformation defined in the text. The energy values for 6 ML films are magnified by factor of 10. The lines serve only as a guide to the eye.

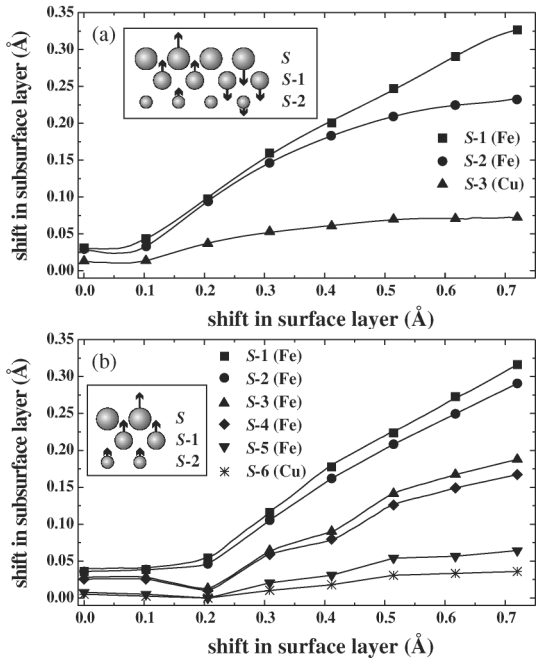

FIG. 4. Deformation of the subsurface layers and of the top layer of the Cu substrate of the 3 ML (a), 6 ML (b) Fe films plotted against the shear deformation of the surface layer. The displacement pattern of the atoms in the deeper layers is sketched in the insets. Note that the atoms are shifted parallel to the surface plane.

and (1×5) reconstructions of 2 and 4 ML Fe/Cu(100) films [14].

As has already been noted, the calculated zigzag distortion by ± 0.59 Å is in excellent agreement with the experimental result of ± 0.65 Å, but substantially larger than the amplitude of the approximately sinusoidal (1×4) and (1×5) reconstructions of 2 and 4 ML films calculated by density functional theory or measured by LEED, namely, 0.25 and 0.20 Å, respectively [5,14]. These older results are not necessarily in contradiction to the new ones — the comparison of the results merely demonstrates that the identification of the true minimum structure by an unconstrained multiparameter relaxation, whether in *ab initio* calculations or by fitting LEED spectra, is an extremely tedious task and does not necessarily lead to the absolute minimum. In the present work the STM results have been used as a guideline for an educated search for the stable film structure with a minimum empirical input. On the other hand, the calculations yield the full three-dimensional film structure which is inaccessible to STM experiments alone.

The shear instability of γ-Fe also explains the $(1 \times 2)_{p2mq}$ reconstruction reported for 6 ML Fe/Cu(001) [5,23], i.e., in regime (ii) with bilayer AFM coupling. Figure 3 displays the variation of the total energy as a function of displacement δ of every second row of atoms in the surface layer along the x direction. A shallow minimum of about 2 meV/Fe atom is found for $\delta = 0.24$ ($\varphi = 13.5°$); thus the atomic displacement is nearly the same as in the (1×4) reconstruction of the thinner layers. In contrast to the 3 ML films, only the surface layer is reconstructed, deeper layers are shifted rigidly, and there is no buckling. The shift of the atoms in the deeper layers, shown in Fig. 4(b), reveals a remarkable pattern: atoms in the $(S - 1)$th and $(S - 2)$th layers, as well as atoms in the $(S - 3)$th and $(S - 4)$th layers, are displaced by almost exactly the same amount. This means that the distances between atoms that couple antiferromagnetically remain about the same as in the nearly isotropic fcc film, shear instability affecting mostly the ferromagnetic bilayers. This is a further manifestation of the correlation between shear instability and magnetism.

In summary, we have demonstrated that tetragonally distorted γ-Fe, which was supposed to represent the correct structure of ultrathin Fe/Cu(001) films in regimes (i) and (ii) is unstable against monoclinic shear deformations in the bulk and in ultrathin films. In the films, the epitaxial constraint limits the shear distortions to narrow domains such that a striped pattern of near-bcc structures results. The shear instability is strongly correlated to the magnetic properties: although the paramagnetic and antiferromagnetic phases of γ-Fe are also unstable against shearing, the shear angle is much smaller than in the ferromagnetic phase, which is stabilized by the shear deformation. In 6 ML films with a bilayer antiferromagnetic ground state, this bilayer sequence is reflected in the atomic displacement pattern. Quite generally, lowering of the total energy by the shear reconstruction is small. This explains the coexistence of the reconstructed and unreconstructed domains and the observation of (1×4), (1×5), and (1×6) modulations. The (1×6) reconstruction may be viewed as resulting from the insertion of an undistorted strip between the two parts of the (1×4) structure in positive and negative directions. The (1×5) pattern observed in LEED (but not in STM) is probably the result of an averaging over (1×4) and (1×6) domains.

This work has been supported by the Austrian Science Funds within Project No. P12753 "Magnetism on the nanometer scale" and through the Center for Computational Materials Science.

[1] B. T. Jonker, K. H. Walker, E. Kisker, G. Prinz, and C. Carbone, Phys. Rev. Lett. **57**, 142 (1986).
[2] W. A. A. Macedo and W. Keune, Phys. Rev. Lett. **61**, 475 (1988).
[3] H. Magnan, D. Chandresis, B. Vilette, O. Heckmann, and J. Lecante, Phys. Rev. Lett. **67**, 859 (1991).
[4] J. Thomassen, F. May, B. Feldmann, M. Wuttig, and H. Ibach, Phys. Rev. Lett. **69**, 3831 (1992).
[5] S. Müller, P. Bayer, C. Reischl, K. Heinz, B. Feldmann, H. Zillgen, and M. Wuttig, Phys. Rev. Lett. **74**, 765 (1995).
[6] R. D. Ellerbrock, A. Fuest, A. Schatz, W. Keune, and R. A. Brand, Phys. Rev. Lett. **74**, 3053 (1995).
[7] D. J. Keavney, D. F. Storm, J. W. Freeland, I. L. Grigorov, and C. Walker, Phys. Rev. Lett. **74**, 4531 (1995).
[8] M. Straub, R. Vollmer, and J. Kirschner, Phys. Rev. Lett. **77**, 743 (1996).
[9] V. L. Moruzzi, P. M. Marcus, and J. Kübler, Phys. Rev. B **39**, 6957 (1989).
[10] T. Kraft, P. M. Marcus, and M. Scheffler, Phys. Rev. B **49**, 11 511 (1994).
[11] R. Lorenz and J. Hafner, Thin Solid Films **281**, 492 (1996); Phys. Rev. B **54**, 15 937 (1996).
[12] T. Asada and S. Blügel, Phys. Rev. Lett. **79**, 507 (1997).
[13] E. G. Moroni, J. Hafner, and G. Kresse, J. Condens. Matter **1**, L35 (1999).
[14] D. Spišák and J. Hafner, Phys. Rev. B **61**, 16 129 (2000).
[15] A. Biedermann, M. Schmid, and P. Varga, Phys. Rev. Lett. **86**, 464 (2001).
[16] J. Giergiel, J. Shen, J. Woltersdorf, A. Kirilyuk, and J. Kirschner, Phys. Rev. B **52**, 8528 (1995).
[17] W. Pitsch, Philos. Mag. **4**, 577 (1959).
[18] G. Kresse and J. Hafner, Phys. Rev. B **48**, 13 115 (1993); G. Kresse and J. Furthmüller, Phys. Rev. B **54**, 11 169 (1996); Comput. Mater. Sci. **6**, 15 (1996); G. Kresse and D. Joubert, Phys. Rev. B **59**, 1758 (1999).
[19] P. Blöchl, Phys. Rev. B **50**, 17 953 (1994).
[20] J. Perdew and A. Zunger, Phys. Rev. B **23**, 5048 (1981).
[21] S. H. Vosko, L. Wilk, and M. Nusair, Can. J. Phys. **58**, 1200 (1980).
[22] J. P. Perdew, J. A. Chevary, S. H. Vosko, K. A. Jackson, M. R. Pedersen, D. J. Singh, and C. Fiolhais, Phys. Rev. B **46**, 6671 (1992).
[23] M. Weinelt, S. Schwarz, H. Beier, S. Müller, L. Hammer, K. Heinz, and Th. Fauster, Phys. Rev. B **63**, 205413 (2001).